MINISTRY OF EDUCATION VIETNAM ACADEMY OF

AND TRAINING SCIENCE AND TECHNOLOGY

GRADUATE UNIVERSITY SCIENCE AND TECHNOLOGY

CAO TRAN NGOC TUAN



DEVELOPMENT OF A TRAJECTORY CONTROL METHOD FOR ELECTRIC WHEELCHAIRS USING HIGHER-ORDER SLIDING MODE CONTROL

SUMMARY OF ELECTRICAL, ELECTRONICS AND TELECOMMUNICATION DOCTORAL THESIS

Major: Control Engineering and Automation

Code: 9 52 02 16

TPHCM, 2025

This thesis is accomplished at: Graduate university Science and Technology - Vietnam Academy of Science and Technology
Supervisors: 1. Supervisors 1: Dr. Truong Nguyen Vu
2. Supervisors 2: Assoc. Prof Ha Quang Phuc
Referee 1:
Referee 2:
Referee 3:
The dissertation is examined by Examination Board of Graduate University of Science and Technology, Vietnam Academy of Science and Technology at (time, date)
The dissertation can be found at: 1. Graduate University of Science and Technology Library 2. National Library of Vietnam

INRODUCTION

1. The necessary of thesis

The demand for electric wheelchairs is increasing rapidly due to various reasons. Specifically, according to statistics, as of 2025, approximately 12% of adults in the United States face mobility limitations, and around 5.5 to 6 million adults use wheelchairs for mobility [1].

To address this issue, automatic or semi-automatic electric wheelchairs have emerged as a solution, enabling users to control the wheelchair more effectively, particularly for those with severe medical conditions who lack the health and flexibility to operate and ensure safety independently.

To develop automated electric wheelchair systems, a core issue that has been extensively studied over the years is trajectory tracking control.

The reason trajectory control is crucial is that electric wheelchairs must operate in relatively complex conditions with numerous uncertainties, including uncertainties in the dynamic model itself. Therefore, a reliable trajectory control method is essential.

In recent years, numerous studies have explored trajectory control solutions for electric wheelchairs [4]-[12]. However, most of these studies fail to fully account for uncertainties or neglect the wheelchair's dynamic model, resulting in a lack of robustness against environmental changes and disturbances. Consequently, their results are often limited to simulations or experiments in controlled laboratory settings. Although some studies have employed Sliding Mode Control [13]-[17] and considered these uncertainties, they remain confined to simulations due to the issue of chattering, which will be discussed in detail in later sections of the thesis.

Therefore, researching a new method for trajectory control of electric wheelchairs that ensures accuracy, robustness against uncertainties, and practical applicability is highly necessary.

2. Research Objective of the Thesis

Develop a trajectory control method for electric wheelchairs using highorder sliding mode control to address the "chattering" issue in sliding mode control, enabling direct practical application.

3. Main Research Content of the Thesis

Design a second-order Terminal Sliding Mode surface, including the ability to calculate the design parameters of the controller and the convergence time of state variables, applicable to practical electromechanical systems.

Design a trajectory controller for the Differential Drive Mobile Robot (DDMR) based on second-order Terminal Sliding Mode.

Apply the controller to a real DDMR system to demonstrate its robustness and effectiveness.

Thesis Content Structure

The thesis consists of 4 chapters:

Chapter 1: Provides an overview of trajectory control studies for electric wheelchairs, DDMR, and in-depth research on sliding mode control, thereby outlining the research direction of the thesis.

Chapter 2: Presents the theory of sliding mode control, existing methods for chattering suppression, and justifies the selection of the main research method in the thesis.

Chapter 3: Introduces and describes the detailed modeling of the DDMR, potential uncertainties, and methods for trajectory control, kinematic control, and dynamic control of the DDMR model.

Chapter 4: Designs a DDMR trajectory controller based on second-order Terminal Sliding Mode, including simulation and experimental results.

Conclusion.

CHAPTER 1: OVERVIEW

1.1 Overview of Related Studies

1.1.1 Studies on Traditional Trajectory Control of Electric Wheelchairs

In 1999, Caracciolo [5] and in 2005, Sun.S [6] utilized the "linearization feedback control" method for trajectory control of mobile robots. Similarly, in 2019, K. Maatoug [7] proposed a trajectory control method based on a Fuzzy controller, and in 2023, A. Amrane [8] suggested a control method using a PID controller. The common limitation of these studies is that they only considered the kinematic model without addressing the dynamic model. Meanwhile, T. Fukao and colleagues [9], as well as Shojaei and colleagues

[10], employed adaptive control, taking into account the dynamic model and the presence of unknown parameters (uncertainties). In 2016, Li.Z [11] used a combined "Neural-Dynamic Optimized Model Predictive" approach, and in 2023, Trujillo [12] proposed a study on "Trajectory Tracking Control of a Mobile Robot using Neural Networks." However, these studies only considered kinematics and were limited to simulations.

1.1.2 Studies on Trajectory Control of Electric Wheelchairs Using SMC

In 2009, Solea [13] proposed a trajectory control study using a conventional SMC sliding surface. Subsequently, several studies applied various SMC sliding surface variants, such as B.B. Mevo [14] in 2018, who used an integral sliding surface, and J. Yang (1999) [15], Lingrong (2011) [16], and Nikranjbar (2018) [17], who proposed methods using first-order SMC. Although these studies achieved good results and accounted for uncertainties, they all encountered the issue of chattering.

1.1.3 Studies on Chattering Suppression in SMC

In 1992, Utkin [20] proposed the "boundary layer" method, which is a simple and widely used approach. The concept of higher-order sliding surfaces was introduced in 1998 by G. Bartolini [22] and Levant [23][24]. In 2006, Ferrara [40] introduced a second-order SMC sliding surface for robotic arms. In 2016, Y. Feng [16] proposed a full-order TSM sliding surface. In 2021, Xinghuo Yu and Yong Feng [41] synthesized SMC methods, specifically focusing on Terminal Sliding Mode Control (TSMC) and higher-order sliding surfaces to reduce chattering. Higher-order TSMC excels in eliminating chattering while maintaining robustness, but it lacks the ability to calculate controller parameters and convergence time, limiting its practical applications. Therefore, this thesis investigates the second-order Terminal Sliding Mode (2TSM) to address these two issues, optimizing chattering suppression for the DDMR system.

1.2 Conclusion

1.2.1 Summary of Current Research Status

1.2.2 Research Issues in the Dissertation

Investigate the design of a second-order Terminal Sliding Mode (2TSM) surface with the capability to calculate controller parameters and convergence time.

Study the design of a trajectory controller for the Differential Drive Mobile Robot (DDMR) based on 2TSM, accounting for model uncertainties.

Conduct experiments on a real DDMR system.

1.2.3 Scope of the Research

The dissertation focuses on the development of a new control algorithm. Therefore, in conducting experiments, the author employs a mobile robot model under scenarios with uncertainties, which facilitates the tuning and modification of the algorithm, rather than performing experiments on a fully developed electric wheelchair.

CHAPTER 2: SLIDING MODE CONTROL THEORY AND CHATTERING SUPPRESSION METHODS

2.1 Asymptotic Stability and Finite-Time Stability

2.1.1 Asymptotic Stability

$$x(t) \to 0$$
 khi $t \to \infty$ (2.1)

***** When uncertainties are present:

If Δf represents unknown disturbance factors, instead of converging to "0", the system's state will converge to:

$$x(t) \to \frac{\Delta f}{\gamma}$$
 khi $t \to \infty$ (2.2)

2.1.2 Finite-Time Stability

$$x(t) \to 0$$
 tại $t = \frac{x(0)^{1-p/q}}{\gamma(1-p/q)},$ (2.3)

Where p, q are odd number and p/q < 1

***** When uncertainties are present:

N If Δf represents unknown disturbance factors:

$$\to x(t) = \left(\frac{\Delta f}{\gamma}\right)^{\frac{q}{p}} \tag{2.4}$$

This means that using a control signal to bring the system to an equilibrium state in finite time will result in a smaller steady-state error compared to asymptotic stability.

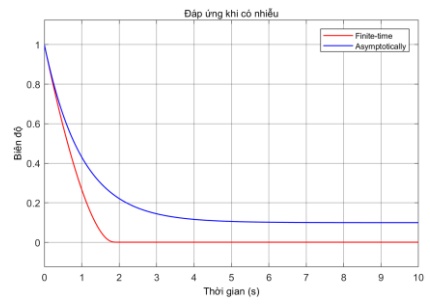


Figure 2.1 System response under uncertainties

$$(\gamma = 1, \Delta f = 0.1, p/q = 1/3)$$

Conclusion: From the above, it can be observed that the control of a system with a "finite-time" response has several advantages over an "asymptotic" response, including:

- Faster convergence speed.
- Higher control accuracy.

Based on these concepts, the thesis will analyze the advantages and disadvantages of linear and nonlinear sliding surfaces in the following section.

2.2 Sliding Mode Control Theory

2.2.1 Linear Sliding Mode (LSM)

Consider the follow system:

$$\begin{cases} \dot{x}_1 = x_2 \\ \dot{x}_2 = f(x) + u + \rho(x, t) \end{cases}$$
 (2.5)

Firstly, the sliding manifold was designed:

$$s = x_2 + \gamma x_1, \gamma > 0 \tag{2.6}$$

when s=0, the system state x_1, x_2 will converge asymptotically to "0" in natural response: $\dot{x}_1 = -\gamma x_1$

The control law was designed as follow:

$$u = u_{eq} + u_n \tag{2.7}$$

where:

$$u_{eq} = -f(x) - \gamma x_2$$

$$u_n = -k sign(s)$$
(2.8)

With the above control law, $s \to 0$ in finite time:

$$t_r = \frac{\sqrt{2}}{\eta} V^{\frac{1}{2}}(0) \tag{2.9}$$

2.2.2 Nonlinear Sliding Mode Manifold

2.2.2.1 Terminal Sliding Mode Control (TSM)

First, the nonlinear manifold was designed as:

$$s = x_2 + \gamma x_1^{p/q}, \gamma > 0 (2.10)$$

With $0 < \frac{p}{q} < 1$ and p, q are odd interger. When s = 0, the state variables x_1, x_2 will converge to "0" according to: $\dot{x}_1 = -\gamma x_1^{p/q}$

The control law was designed as follow:

$$u = u_{eq} + u_n$$

$$u_{eq} = -f(x) - \gamma p / q x_1^{p/q-1} \dot{x}_1$$

$$u_n = -k sign(s)$$
(2.11)

Remark: in the control signal: $ueq = -f(x) - \gamma \frac{p}{q} x_1^{\frac{p}{q}-1} \dot{x}_1$ has the possibility of encountering a singularity poin $x_1 = 0$, $\dot{x}_1 \neq 0$. Figure 2.2 (t = 0.37s).

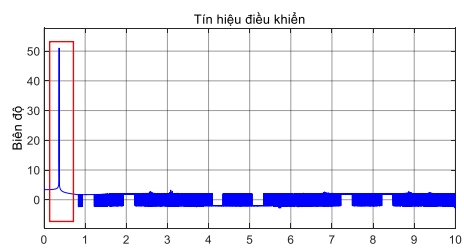


Figure 2.2 the control signal with singularity point

2.2.2.2 Nonsingular Terminal Sliding Mode Control (NTSM)

$$s = x_1 + \frac{1}{\nu} x_2^{q/p} \tag{2.12}$$

When s = 0, the response of NTSM (2.12) equivalent to (2.10). The control law $u = u_{eq} + u_n$ was designed as follow:

$$\begin{cases} u_{eq} = -f(x) - \gamma \frac{p}{q} x_2^{2-q/p} \\ u_n = -k sign(s) \end{cases}$$
 (2.13)

Applied the control law (2.13), it gets:

$$\dot{V} = s \frac{1}{\gamma} \frac{q}{p} x_2^{\frac{q}{p} - 1} (-k sign(s) + \rho(t))$$

Conclusion: Control signal $u_{eq} = -f(x) - \gamma \frac{p}{q} x_2^{2-q/p}$ was eliminated the singularity point at $x_2 = 0, x_1 \neq 0$.

The inherent disadvantage of Sliding Mode Control (SMC) is the phenomenon of "chattering." Research efforts aimed at eliminating this "chattering" phenomenon will be presented in the following section.

2.3 Eliminating "chattering" in sliding mode control

2.3.1 Method using the saturation function

2.3.2 Method using the sigmoid function

2.3.3 Higher-order sliding mode method

2.3.3.1 Higher-order LSM sliding surface

The sliding manifold is proposed:

$$s = \ddot{x} + \alpha \dot{x} + \beta x \tag{2.14}$$

Control law $u = u_{eq} + u_n$ is designed as follow:

$$\begin{cases} u_{eq} = -f(x) - \alpha \dot{x}_1 - \beta x_1 \\ \dot{u}_n = -k sign(s) \end{cases}$$
 (2.15)

Ex: We design the sliding surface and control signal as follows:

$$s = \ddot{x}_1 + 2\dot{x}_1 + x_1$$
$$u = 0.1x_2 - 2\dot{x}_1 - x_1 - 5\int_0^t sign(s)dt$$

The simulation results are shown in Figure 2.3.

It can be observed that although the control signal is smooth and chattering is eliminated, the drawback of the linear sliding surface remains: the state variable does not reach zero but only converges asymptotically.

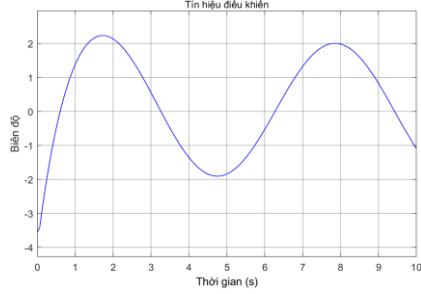


Figure 2.3 Control signal

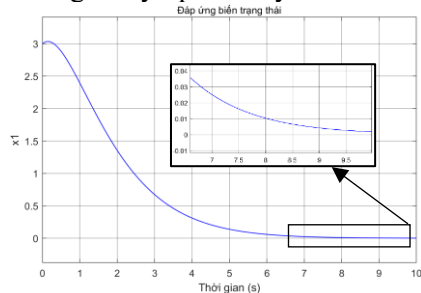


Figure 2.4 State response

2.3.3.2 Full order Terminal Sliding Mode (FOTSM)

According to [23], the sliding surface is chosen as follows:

$$s = \dot{x}_n + c_n sgn(x_n)|x_n|^{\alpha_n} + \dots + c_1 sgn(x_1)|x_1|^{\alpha_1}$$
 (2.16)

where c_i , α_i (i = 1, 2, ... n) are constant. c_i is chosen such as $p^n + c_n p^{n-1} + \cdots + c_2 p + c_1$ is Hurwitz, and α_i is chosen as follows

$$\begin{cases} \alpha_{1} = \alpha, & n = 1 \\ \alpha_{i-1} = \frac{\alpha_{i}\alpha_{i+1}}{2\alpha_{i+1} - \alpha_{i}}, & i = 1, 2, ..., n \ \forall n \ge 2 \end{cases}$$
 (2.17)

Where: $\alpha_{n+1} = 1$, $\alpha_n = \alpha$, $\alpha \in (1 - \varepsilon, 1)$, $\varepsilon \in (0,1)$.

Applying it to system (2.5), we obtain the sliding surface:

$$s = \ddot{x}_1 + c_2 sign(\dot{x}_1) |\dot{x}_1|^{\alpha_2} + c_1 sign(x_1) |x_1|^{\alpha_1}$$
 (2.18)

Control law $u = u_{eq} + u_n$ is designed as follow:

$$u_{eq} = -f(x) - c_2 sign(\dot{x}_1)|\dot{x}_1|^{\alpha_2} - c_1 sign(x_1)|x_1|^{\alpha_1}$$

$$\dot{u}_n + \lambda u_n = v; v = -(k_d + k_T + \eta) sign(s)$$
(2.19)

Example: Consider the same system as above. We design the sliding surface and control signal as follows:

$$s = \ddot{x}_1 + 2sign(\dot{x}_1)|\dot{x}_1|^{9/16} + sign(x_1)|x_1|^{9/23}$$

$$\to u = u_{eq} + e^{-0.1t} \int_0^t e^{-0.1t} v dt$$

Where e is the base of the natural logarithm. (ln (e) = 1).

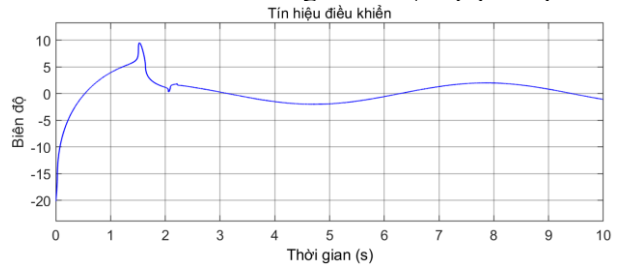


Figure 2.5 Control signal FOTSM

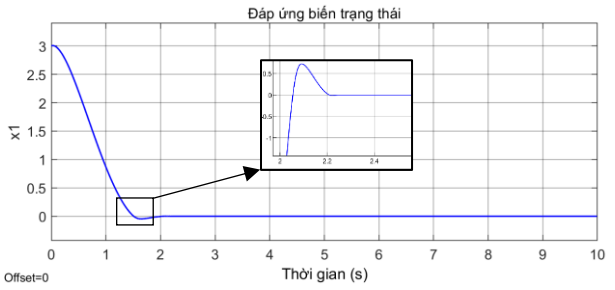


Figure 2.6 State response FOTSM

It can be observed that the control signal has almost completely eliminated chattering (Figure 2.5) and the state variable has converged to zero (Figure 2.6). However, this method currently has two major issues that prevent its practical application [24][40]: it cannot be computed and it cannot be measured.

2.4 Conclusion

The FOTSM method is the optimal approach to eliminate chattering in sliding mode control, provided that the existing drawbacks can be overcome.

CHAPTER 3. MOBILE ROBOT AND TRAJECTORY CONTROL METHOD

3.1 Introduction the model

3.1.1 Kinematic model

***** Forward kinematic:

$$\begin{cases} v = \frac{v_r + v_l}{2} = \frac{R(\dot{\varphi}_r + \dot{\varphi}_l)}{2} \\ \omega = \frac{v_r - v_l}{2L} = \frac{R(\dot{\varphi}_r - \dot{\varphi}_l)}{2L} \end{cases}$$
(3.1)

❖ Inverse kinematic:

$$\begin{cases} v_r = v + \omega L \\ v_l = v - \omega L \end{cases}$$
 (3.2)

3.1.2 Dynamic model

$$\left(m + \frac{2}{R^2} I_w\right) \dot{v} - m_c d\omega^2 = \frac{1}{R} (\tau_r + \tau_l)$$

$$\left(I + \frac{2L^2}{R^2} I_w\right) \dot{\omega} + m_c d\omega v = \frac{L}{R} (\tau_r - \tau_l)$$
(3.3)

3.1.3 Uncertainties in the model

- Uncertainty about the mass: limited to 50 100 (kg)
- Change in the center of mass: limited to $\Delta d = 15$ (cm)

$$M_0 \begin{bmatrix} \dot{v} \\ \dot{\omega} \end{bmatrix} = V_0 + C \begin{bmatrix} \tau_r \\ \tau_l \end{bmatrix} \underbrace{+\Delta V - \Delta M \begin{bmatrix} \dot{v} \\ \dot{\omega} \end{bmatrix} + d(t)}_{\rho(t)}$$
(3.4)

Where M_0 , V_0 are the known initial values, ΔM and ΔV are the changing quantities, d(t) is other uncertainties, $\rho(t)$ is the total uncertainties values.

3.2 Trajectory control method

Based on the pre-designed trajectory, the reference DDMR will move ahead, and the actual DDMR will follow. The control diagram is shown in Figure 3.1.

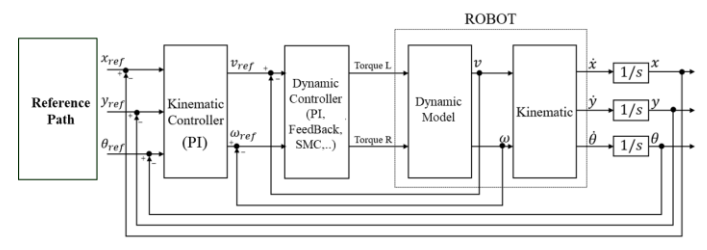


Figure 3.1 Trajectory control diagram

***** Kinematic Controller:

The tracking error p_e is the different between real and refference position, denoted as $p = [x \ y \ \theta]^T$ and the refference position, denoted as $p_{ref} = [x_{ref} \ y_{ref} \ \theta_{ref}]^T$, it obtain:

$$p_e = \begin{bmatrix} x_e \\ y_e \\ \theta_e \end{bmatrix} = p_{ref} - p = \begin{bmatrix} x_{ref} - x \\ y_{ref} - y \\ \theta_{ref} - \theta \end{bmatrix}$$
(3.5)

The outermost kinematic controller uses a simple P-type controller, designed as follows:

$$\omega_{ref} = K_w. \theta_e, v_{ref} = K_v. d_e \tag{3.6}$$

where ω_{ref} , v_{ref} are the refference velocities; K_w , K_v are the gain controller; $d_e = (x_e^2 + y_e^2)^{1/2}$ và $\theta_e = tan^{-1}(y_e, x_e)$.

Dynamic Controller:

After the signals ω_{ref} , v_{ref} are sent to the dynamic controller, it calculates and generates the control signals—torques τ_{right} , τ_{left} - to each wheel (Figure 3.2).

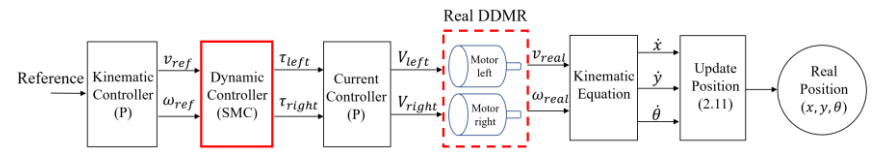


Figure 3.2 Trajectory control flowchart in simulation

3.3 Trajectory Controller Based on Linear Sliding Mode (LSM)

3.3.1 Design of Trajectory Controller Using LSM Sliding Surface

$$M\ddot{q} = V(\dot{q}) + Cu(t) + \rho(t) \tag{3.7}$$

The error is defined as:

$$\dot{e}(t) = \dot{q} - \dot{q}_r = [v_e, \, \omega_e]^T = [v - v_{ref}, \, \omega - \omega_{ref}]^T$$
 (3.8)

Sliding manifold: $s = \dot{e} + \gamma e$

Theorem 1: The control law is: $u = u_{eq} + u_n$

$$u_{eq} = C^{-1}M(-M^{-1}V(\dot{q}) + \ddot{q}_r - \gamma \dot{e})$$
(3.9)

$$u_n = -C^{-1}Msign(s)(k+\eta)$$
(3.10)

3.3.2 Simulation

3.3.2.1 LSM without "boundary layer"

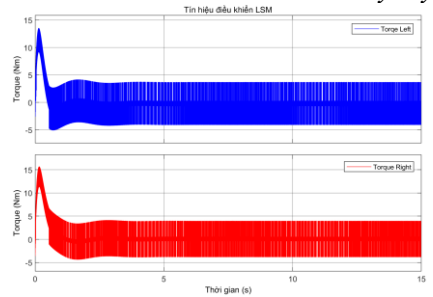


Figure 3.3 Trajectory 1 control signal (without boundary layer)

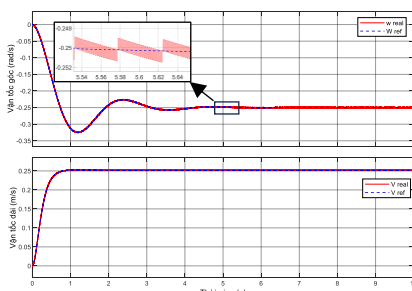


Figure 3.4 Velocities response (trajectory 1 - without boundary layer)

LSM with boundary layer 3.3.2.2

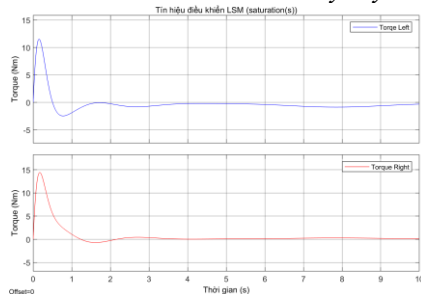


Figure 3.5 Trajectory 1 control signal (with boundary layer)

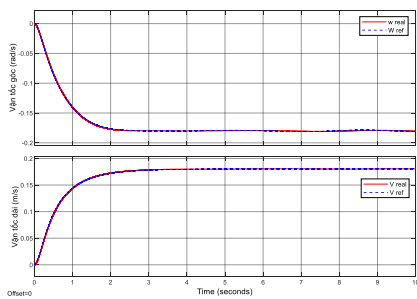


Figure 3.6 Velocities response (trajectory 1 - with boundary layer)

3.3.2.3 Comment

It can be clearly observed that the use of a boundary layer significantly reduces the accuracy of the controller.

Trajectory controller using NTSM 3.4

Design trajectory controller using NTSM 3.4.1

$$s = e + \frac{1}{\gamma} \dot{e}^{q/p} \tag{3.11}$$

Theorem 2: Control law is: $u = u_{eq} + u_n$

Where:

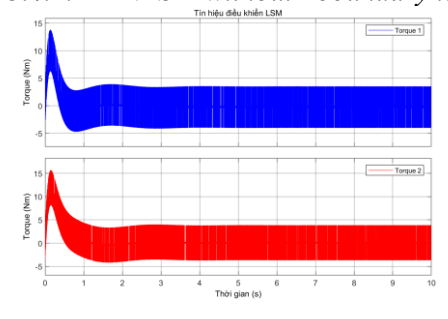
$$u_{eq} = C^{-1}M\left(-M^{-1}V(\dot{q}) + \ddot{q}_r - \gamma \frac{p}{q}\dot{e}^{2-q/p}\right)$$
(3.12)

$$u_n = -C^{-1}Msign(s)(k+\eta)$$
(3.13)

 $u_n = -C^{-1}Msign(s)(k+\eta)$ And satisfied the condition: $k = Max\{||M^{-1}\rho(t)||\}$, $\eta > 0$

3.4.2 Simulation

3.4.2.1 NTSM without "boundary layer"



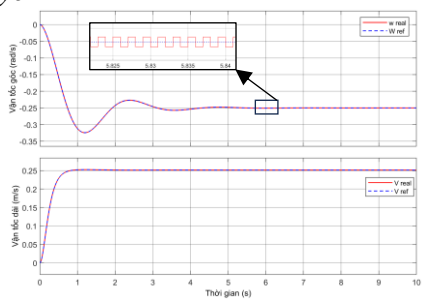


Figure 3.7 Trajectory 1 control signal (NTSM without boundary layer)

Figure 3.8 Velocities response (trajectory 1 – NTSM without boundary layer)

3.4.2.2 Mô phỏng NTSM với boundary layer

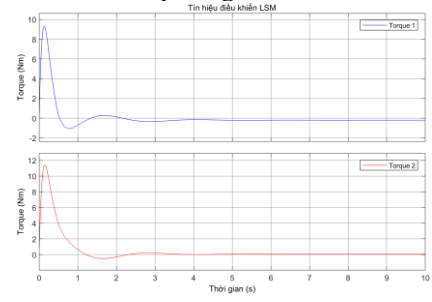


Figure 3.9 Trajectory 1 control signal (NTSM with boundary layer)

Figure 3.10 Velocities response (trajectory 1 – NTSM with boundary layer)

3.4.2.3 Comment.

It is observed that NTSM demonstrates superiority over LSM in ensuring accuracy, convergence speed, and robustness.

3.5 Conclusion

The chattering phenomenon appears in both LSM and NTSM methods, and the "boundary layer" has shown a lack of robustness and reduced controller accuracy. Therefore, in Chapter 4, the dissertation will address this issue using the higher-order sliding mode method.

CHAPTER 4: DESIGN OF TRAJECTORY CONTROLLER USING SECOND-ORDER TERMINAL SLIDING MODE METHOD

4.1 Second order TSM

4.1.1 Convergence Time Characteristics of the Sliding Surface

The second order TSM manifold is chosen as follow:

$$s = \ddot{x} + \gamma_1 \dot{x}^\alpha + \gamma_2 x^\beta \tag{4.1}$$

Wherein, the following conditions are satisfied:

$$0 < \alpha = \frac{q}{p} < 1, \beta = \frac{\alpha}{2-\alpha} = \frac{q}{2p-q}, p > q \text{ are odd intergers};$$

$$0 < \gamma_1; \quad \gamma_2 = \gamma_1^{\beta+1} \frac{\alpha^{\beta}}{(\beta+1)^{\beta}} \left(1 - \frac{\alpha}{2}\right) > 0;$$

$$x(0) = x_0, \dot{x}(0) = -\gamma_1^{\beta/\alpha} \left(\frac{\alpha}{\beta+1}\right)^{\beta/\alpha} x_0^{1/(2-\alpha)}.$$

$$(4.2)$$

Theorem 3: when the manifold **Error! Reference source not found.** c onverge to 0 (s = 0) and the conditions (4.2) is satisfied, the state variable x(t) and its derivative $\dot{x}(t)$ converge to 0 in finite time, which is calculated as follow:

$$t_{convergence} = \frac{\alpha}{\alpha - \beta} \left(\frac{\gamma_1 \alpha}{\beta + 1} \right)^{-\beta/\alpha} \chi_0^{(\alpha - \beta)/\alpha}$$
 (4.3)

Prove:

Take $y = \dot{x} \rightarrow \ddot{x} = y \frac{dy}{dx}$, s = 0, (4.1) become: $F(y, \dot{y}) = y \frac{dy}{dx} + \gamma_1 y^{\alpha} = -\gamma_2 x^{\beta}$ (4.4)

natural response of (4.4) is:

$$F(y, \dot{y}) = y \frac{dy}{dx} + \gamma_1 y^{\alpha} = 0 \tag{4.5}$$

Where y = 0 is particular solution of (4.5), in the case $y \neq 0$, (4.5) is rewritten as: $y^{1-\alpha}dy = -\gamma_1 dx$.

Integrating both sides, we obtain:

$$\frac{1}{2-\alpha}y^{2-\alpha} = -\gamma_1 x + C$$

$$y = (Mx + N)^{1/(2-\alpha)}$$
(4.6)

With the presence of the signal $u = -\gamma_2 x^{\beta}$, the general solution has the form:

$$y = (Mx + f(x))^{1/(2-\alpha)}$$
 (4.7)

Where N = f(x) is the function of x. Substituting (4.7) into (4.4), we obtain:

$$\left(\gamma_1 + \frac{M + \frac{df}{dx}}{2 - \alpha}\right) \left(Mx + f(x)\right)^{\beta} = -\gamma_2 x^{\beta}$$
(4.8)

where

- Mx + f(x) has the form Mx + f(x) = Kx; derive f(x) = (K - M)x

$$-\frac{df}{dx} = (K - M)$$

Equating both sides, we obtain:

$$\left(\gamma_1 + \frac{K}{2 - \alpha}\right) K^{\beta} = -\gamma_2 \tag{4.9}$$

From (4.9), it easy to see: if $\gamma_2 > 0$, K < 0, then:

- The minimum of $g(K) = \left(\gamma_1 + \frac{K}{2-\alpha}\right)K^{\beta} + \gamma_2$ exits at $K^* = -\gamma_1 \frac{\beta(2-\alpha)}{\beta+1} = -\gamma_1 \frac{\alpha}{\beta+1}$
- $g\left(K^* = -\gamma_1 \frac{\alpha}{\beta + 1}\right) = 0$ and K^* is the unique solution of (4.9)

The result is:

$$y = (K^*x)^{1/(2-\alpha)} = \underbrace{-\left[\gamma_1 \frac{\alpha}{\beta+1}\right]^{1/(2-\alpha)}}_{A} x^{1/(2-\alpha)}$$

Then, the general solution is

$$y = \dot{x} = Ax^{1/(2-\alpha)} \tag{4.10}$$

Remark : Picard – Lindelöf theorem assert that (4.10) is the unique solution of the equation. $F(y, \dot{y}) = y \frac{dy}{dx} + \gamma_1 y^{\alpha} = -\gamma_2 x^{\beta}$ according to the given initial conditions.

Hoàn tất chứng minh.

4.1.2 Simulation of sliding surface convergence time:

With $\gamma_1, \gamma_2, \alpha, \beta$ are chosen in theorem 3, the desire convergence time is t = 2s, the sliding manifold is designed as follow:

$$s = \ddot{x} + 9.92\dot{x}^{3/5} + 12.8x^{3/7} = 0 \tag{4.11}$$

With the initial variable $x_0 = 5$, the systems response as in Figure 4.1:

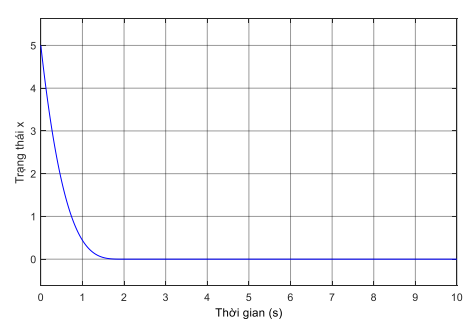


Figure 4.1 Simulation results of the natural convergence of the 2TSM surface.

4.2 Trajectory Control Based on Second-Order TSM Sliding Surface

4.2.1 Controller Design

Theorem 4: The velocity error of the system will converge to zero when the control signal is designed as follows: $u = u_{eq} + u_n$

$$u_{eq} = C^{-1}M(-M^{-1}V + \ddot{q}_r - \gamma_1 \dot{e}^{\alpha} - \gamma_2 e^{\beta})$$
 (4.12)
$$\dot{u}_n = C^{-1}M(sign(s)(k+\eta))$$

Where $k = Max\{||M^{-1}\dot{\rho}(t)||\} \text{ và } \eta > 0$

Prove:

By substituting the system state errors into the 2TSM sliding surface (4.12), we obtain:

$$s = M^{-1}(V(\dot{q}) + C\tau(t) + \rho(t)) - \ddot{q}_r + \gamma_1 \dot{e}^{\alpha} + \gamma_2 e^{\beta}$$

Substituting the control signal (4.12) into the above expression:

$$s = M^{-1}Cu_n + M^{-1}\rho(t)$$

Consider Lyapunov function: $V = 0.5s^{T}s$, it gets:

$$\dot{V} = s^T \dot{s} = s^T \left(-sign(s)k - sign(s)\mu + M^{-1}\dot{\rho}(t) \right) \tag{4.13}$$

It follow that:

$$\begin{split} \dot{V} & \leq -k\|s\| - \eta\|s\| + M^{-1}\dot{\rho}(t) \leq -\eta\|s\| = -\eta\sqrt{2}V^{1/2} < 0 \\ s & \to 0 \text{ in finite time } t_r \leq \frac{\sqrt{2}V^{1/2}(0)}{\eta} \,. \end{split}$$

This completes the proof.

4.2.2 Simulation

The sliding surface and control signal are designed as follows:

$$s = \ddot{e} + 4\dot{e}^{3/5} + 3.49e^{3/7}$$

$$\begin{split} u_{eq} &= C^{-1}M\left(-M^{-1}V + \ddot{q}_r - 4\dot{e}^{\frac{3}{5}} - 3.49e^{\frac{3}{7}}\right)\\ \dot{u}_n &= C^{-1}M\left(sign(s)([2;1]^T + 0.2)\right) \end{split}$$

The simulation results from Figure 4.3 to Figure 4.6.

• **Trajectory 1:** circle with a radius of 1 meter.

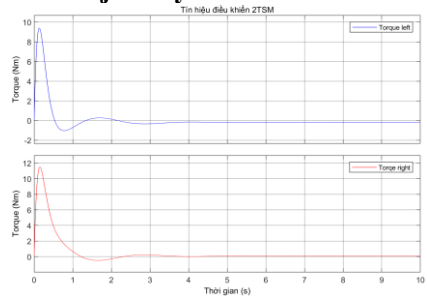


Figure 4.2 Trajectory 1 – control signal (2TSM)

Figure 4.3 Trajectory 1 – velocities response (2TSM)

It can be seen that the 2TSM controller has eliminated the chattering phenomenon in the control signal (Figure 4.3) while maintaining high accuracy.

• **Trajectory 2:** A path consisting of straight segments combined with 90° turns.

For trajectory 2, the 2TSM controller still demonstrates robustness and high accuracy (Figure 4.6).

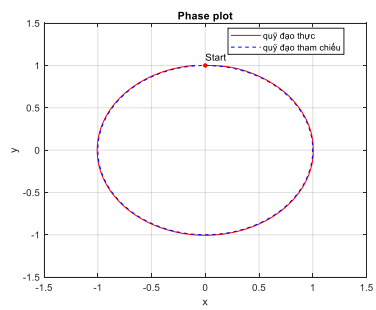


Figure 4.4 DDMR result in trajectory 1(2TSM)

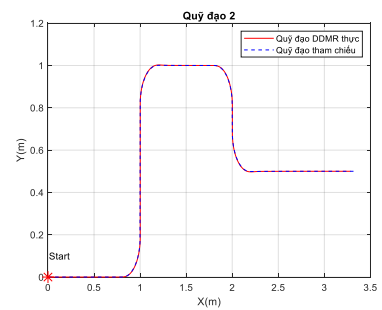


Figure 4.5 DDMR result in trajectory 2 (2TSM)

4.3 Experiment

4.3.1 DC motor control

4.3.1.1 Simulation

From the simulation, it can be seen that all four control methods exhibit comparable responses, each bringing the system to a convergent state in approximately 1 second. Among them, the 2TSM method (Figure 4.10) demonstrates superior performance by ensuring high accuracy, driving the error to zero, and eliminating chattering.

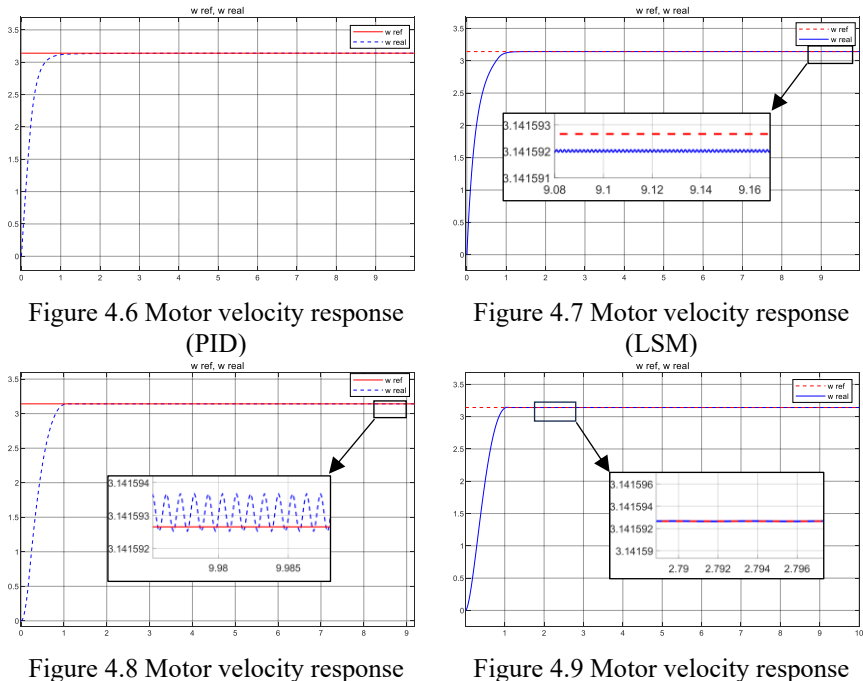
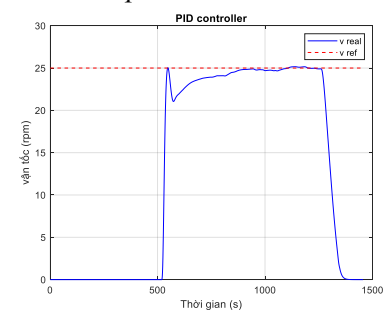


Figure 4.8 Motor velocity response (NTSM)

Figure 4.9 Motor velocity response (2TSM)

4.3.1.2 Experiment



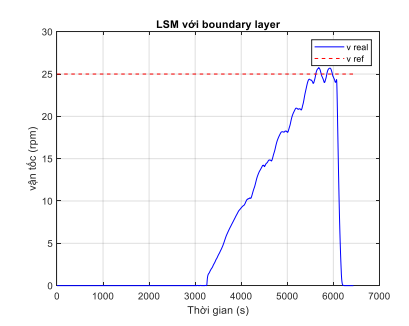


Figure 4.10 PID Controller

Figure 4.11 LSM ($\varepsilon = 0.01$)

Through the above experiments and simulations, the thesis has demonstrated the outstanding advantages of 2TSM in maintaining the characteristic robustness of SMC, the high accuracy of TSM, and the ability to eliminate chattering for direct application in practical control systems, forming the basis for applying it to trajectory control experiments.

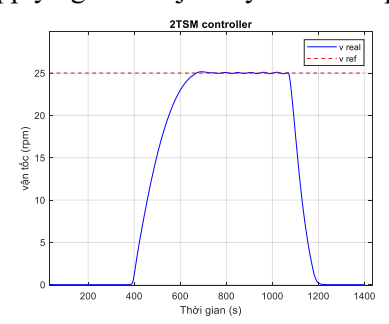


Figure 4.12 2TSM controller

4.3.2 Trajectory Control

4.3.2.1 Simulation

Before conducting trajectory control experiments, the thesis briefly presents the simulation results of 2TSM compared with NTSM and NTSM using a boundary layer on the same reference system (with identical uncertainties and physical parameters of the DDMR) to more clearly evaluate the superiority of the 2TSM method using specific metrics.

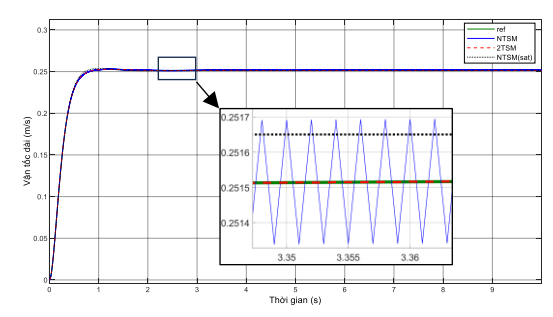


Figure 4.13 Long-term velocity response results of the three methods.

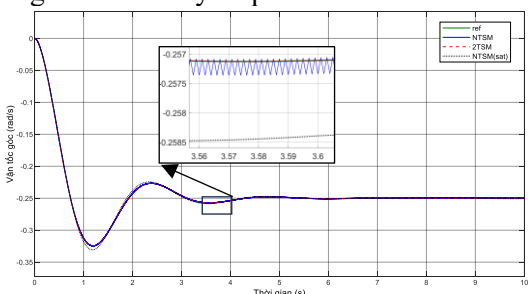


Figure 4.14 Angular velocity response (Rad/s)

4.3.2.2 Experiment

<u> Бхрегинені</u>	
Dimension (DxRxC)	20x20x20 cm
Wheel radius	6 cm
Wheelbase distance	23.5 cm
Power (DC)	12VDC 6000mah

> Trajectory 1: Trajectory 1 consists of straight paths; the experimental results are shown in Figure 4.16.

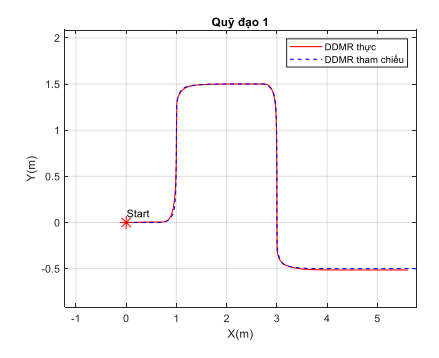


Figure 4.15 The DDMR moves along trajectory 1.

Trajectory 2: Trajectory 2 consists of diagonal paths, followed by a return to the starting position; the experimental results are shown in Figure 4.17.

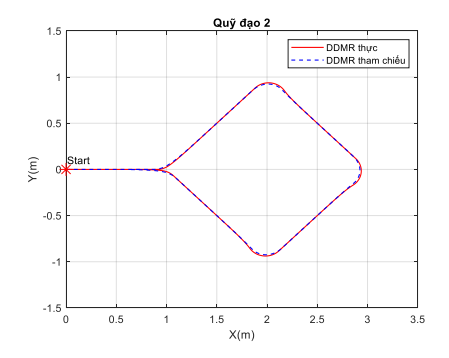


Figure 4.16 The DDMR moves along trajectory 2

➤ **Trajectory 3:** Trajectory 3 is a circle with a radius of 1 meter. The experimental results are shown in Figure 4.18.

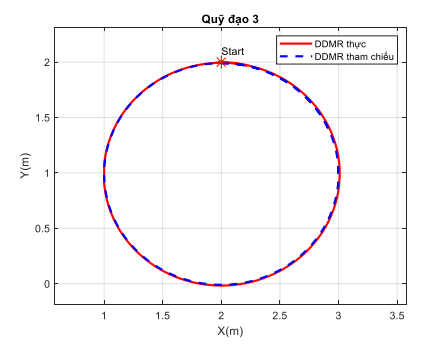


Figure 4.17 The DDMR moves along trajectory 3

4.4 Conclusion:

The trajectory control method based on 2TSM, as designed in Chapter 4, has fully met the requirements set forth in the thesis, as demonstrated through both simulations and experiments.

CONCLUSION

Main Research Contents of the Thesis

The thesis focuses on studying the order-raising solution for nonlinear sliding surfaces to overcome the chattering phenomenon while maintaining advantages such as robustness against uncertainties and high accuracy.

In Chapter 2, the thesis presents the theoretical foundation of sliding mode control, emphasizing the analysis of the advantages and disadvantages of traditional sliding mode control methods and chattering elimination solutions. This leads to the decision to raise the order of the TSM sliding surface to leverage its benefits while generating smooth control signals applicable in practical electromechanical systems.

New Scientific Contributions of the Thesis

The thesis has two main contributions:

- ➤ Designing a complete second-order Terminal Sliding Mode (TSM) sliding surface with the capabilities to:
 - Eliminate chattering in the control signal
 - Maintain the robustness characteristic of SMC

- Ensure state convergence to the equilibrium point within finite time
- Allow computation of controller parameters
- Enable measurement of the state response time
- ➤ Designing a trajectory (dynamic) controller for the DDMR system, taking into account model uncertainties and unknown disturbances.

Among the thesis results, two very important points that have not been addressed by other studies are: the ability to compute the controller parameters and measure the state response time of the 2TSM method.

Research direction of the dissertation:

Develop a complete solution for an autonomous electric wheelchair system that can move within designated areas within the campus.

LIST OF THE PUBLICATIONS RELATED TO THE DISSERTATION

- 1. TNT Cao, TB Pham, TN Nguyen, DL Vu, & NV Truong, 2024, Second-Order Terminal Sliding Mode Control for Trajectory Tracking of a Differential Drive Robot. Mathematics, 12(17), 2657
- 2. TNT Cao, TB Pham, DH Tran, XL Gia, TN Nguyen and NV Truong, 2024, Non-singular terminal sliding mode control for trajectory-tracking of a differential drive robot. E3S Web of Conferences 496, 02005
- 3. Thanh Binh Pham, TNT Cao, Tan No Nguyen and Nguyen Vu Truong, 2025, Adaptive Full Order Sliding Mode Control for Electrical Motor Drive, International Conference on Energy, Infrastructure and Environmental Research (EIER 2025).
- 4. Dang-Phuc Tran, TNT Cao, Duc-Hieu Tran, Tan-No Nguyen and Nguyen-Vu Truong, 2025, Electrical motor drive parameter estimation via higher order sliding mode control, International Conference on Energy, Infrastructure and Environmental Research (EIER 2025).